Singularity-free interpretation of the thermodynamics of supercooled water

Srikanth Sastry,[1,*] Pablo G. Debenedetti,[2] Francesco Sciortino,[3] and H. E. Stanley[4]
[1]*Physical Sciences Laboratory, Division of Computer Research and Technology, National Institutes of Health, Bethesda, Maryland 20952*
[2]*Department of Chemical Engineering, Princeton University, Princeton, New Jersey 08544*
[3]*Dipartimento di Fisica, Universitá di Roma La Sapienza and Istituto Nazionale per la Fisica della Materia, Piazzale Aldo Moro 2, Rome 00185, Italy*
[4]*Center for Polymer Studies and Department of Physics, Boston University, Boston, Massachusetts 02215*
(Received 10 January 1996)

The pronounced increases in isothermal compressibility, isobaric heat capacity, and in the magnitude of the thermal expansion coefficient of liquid water upon supercooling have been interpreted either in terms of a continuous, retracing spinodal curve bounding the superheated, stretched, and supercooled states of liquid water, or in terms of a metastable, low-temperature critical point. Common to these two scenarios is the existence of singularities associated with diverging density fluctuations at low temperature. We show that the increase in compressibility upon lowering the temperature of a liquid that expands on cooling, like water, is not contingent on any singular behavior, but rather is a thermodynamic necessity. We perform a thermodynamic analysis for an anomalous liquid (i.e., one that expands when cooled) in the absence of a retracing spinodal and show that one may in general expect a locus of compressibility extrema in the anomalous regime. Our analysis suggests that the simplest interpretation of the behavior of supercooled water consistent with experimental observations is free of singularities. We then develop a waterlike lattice model that exhibits no singular behavior, while capturing qualitative aspects of the thermodynamics of water. [S1063-651X(96)03406-X]

PACS number(s): 64.70.Ja, 05.70.Ce, 64.60.My

I. INTRODUCTION

At ambient pressures and temperatures, many properties of water exhibit anomalous behavior. These include the well-known density maximum at 4 °C at atmospheric pressure, the rapid increase upon cooling of the isothermal compressibility and the constant pressure specific heat, and quantities related to the microscopic dynamics. These anomalies are strongly enhanced as the temperature is lowered below the melting temperature. Hence, a significant part of studies aimed at elucidating the anomalous behavior of water have been conducted in the supercooled regime.

It is well established that the microscopic origin of the anomalies is related to increased hydrogen bonding between water molecules as the temperature is lowered. However, the thermodynamic properties that result from the microscopic behavior, dictated by the hydrogen bonding interactions, are not well established. Specifically, there are two different thermodynamic scenarios that have been proposed for the metastable behavior of water, which invoke distinct thermodynamic mechanisms for an explanation of anomalous behavior (Fig. 1).

(i) *Retracing spinodal scenario.* The stability limit conjecture (SLC), proposed by Speedy [1,2], attributes the anomalous behavior on supercooling to the presence of a spinodal instability at low temperatures, causing divergences in the response functions as the spinodal temperature is approached. In addition, the spinodal that is present at low temperatures (and positive pressures) is argued to be the liquid-gas spinodal that retraces to higher pressure values below a temperature at which it intersects the locus of density maxima [or, temperature of maximum density (TMD)] in the (P,T) plane. Speedy [1,2] (and later, in a more general context, Debenedetti and D'Antonio [3–6]) showed that if one assumes that the TMD [which at ambient conditions is negatively sloped in the (P,T) plane] remains negatively sloped at negative pressures, the inevitable intersection of the TMD and the liquid-gas spinodal results in a retracing of the spinodal as a consequence of thermodynamic consistency alone. However, there is no clear argument necessitating such a retracing spinodal to reach positive pressures. An experimental verification of the SLC is difficult, since the nucleation of ice prevents measurements at low enough temperatures to obtain an unequivocal signature of the presence of the spinodal.

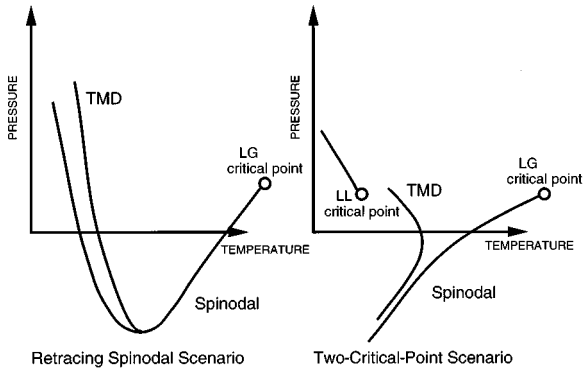

FIG. 1. Schematic representation of (a) the retracing spinodal and (b) two-critical-point scenarios. Note that in the two-critical-point scenario, apart from the usual liquid-gas (LG) critical point, one has in addition a metastable liquid-liquid (LL) critical point.

*Present address: Department of Chemical Engineering, Princeton University, Princeton, NJ 08544. Electronic address: sastry@eyor.princeton.edu

(ii) *Critical-point scenario.* Poole *et al.* [7,8] attempted to calculate the location of the liquid-gas spinodal in computer simulations of water with commonly used model potentials. They failed to observe the retracing of the spinodal. The slope of the TMD does not remain negative, but changes sign at negative pressures, thus removing the thermodynamic requirement for the spinodal to retrace [9]. In addition to the absence of retracing of the spinodal, Poole *et al.* also observed that the isotherms of the highly supercooled liquid calculated in simulation showed inflections at positive pressures, with the inflections growing more pronounced at lower temperatures, suggesting the possibility that the inflections may develop into a critical point at some low temperature. The scenario developed by Poole *et al.*, based on an extrapolation of simulation data (*critical point scenario*), ascribes the anomalous properties of metastable water to the presence of a metastable, low-temperature liquid-liquid critical point, associated with a phase transition between a low-density and a high-density liquid phase. Further support for this interpretation has been offered through an analysis of the experimentally observed apparent first order transitions between the low density and high density forms of amorphous ice [10–14].

Extensive thermodynamic analysis for the retracting spinodal scenario has been carried out in the past [1–6]. It has been shown by purely thermodynamic arguments that the density maximum line, if negatively sloped in the (P,T) plane, intersects the liquid-gas spinodal line in the negative pressure region, causing the spinodal line to retrace toward positive pressures [1].

Less effort has been devoted to the description of the thermodynamic constraints imposed by the existence of a negatively-sloped TMD in the absence of a retracing liquid-gas spinodal. In this paper we initiate such an analysis for the retracing-TMD scenario (Sec. II). We show that, independently of any proposed scenario, the increase of the isothermal compressibility K_T on cooling below a negatively sloped TMD line is a requirement of thermodynamics. We therefore argue that the increase in K_T on cooling, although consistent with both proposed scenarios, cannot be invoked to support either the retracing spinodal or the existence of a critical point. We also show that the retracing TMD observed in molecular dynamics simulations arises as a necessary feature of the phase diagram, when the spinodal is not retracing. The locus of K_T extrema in the (P,T) plane, which we call the ''locus of temperatures of extremal compressibility'' (or TEC locus), plays a significant role in this analysis, and may potentially offer a way of distinguishing between possible metastable behaviors. However, no further constraints may be derived from a purely thermodynamic analysis on the behavior of an anomalous fluid at low temperatures.

Both scenarios described above have tacitly assumed that some form of critical behavior is necessary to explain the anomalous behavior of response functions in water. As we shall argue below, anomalous properties and any critical behavior that may occur in an anomalous fluid are independent issues. In the context of the retracing-TMD scenario, it is thus important to understand thoroughly which observed properties are necessarily related to critical behavior and which properties are not. Towards this goal, we develop in Sec. III a simple lattice model that displays the general features of an anomalous fluid without a retracing spinodal. We study a specific version of the model that does not permit any cooperativity between hydrogen bond forming regions. The model displays inflections in $P(V)$ as observed in the molecular dynamics study of water. However, the inflections do not fully develop into a second critical point. Aside from the interest for the modeling of fluids with a TMD locus, the model studied in this work is of inherent interest from a formal thermodynamic viewpoint in that the partition function evaluation needs to be carried out in the *generalized ensemble*, specified by thermodynamic variables that are all intensive [15].

In Sec. IV, we discuss the conclusions that may be drawn from the present work and possible directions for future research suggested by the results presented here.

II. THERMODYNAMIC ANALYSIS

In Sec. II A, we first derive a general relation between the slope of the TMD locus and the isobaric temperature dependence of K_T. This relation applies to all anomalous fluids, and we discuss its importance in the case of water. In Sec. II B, we analyze the thermodynamic constraints on the behavior of an anomalous fluid in the absence of a retracing spinodal and derive the possible behaviors that satisfy these constraints.

A. Relationship between temperature dependence of K_T and the TMD

We begin by finding the constraint imposed on the isothermal compressibility,

$$K_T \equiv -\frac{1}{v}\left(\frac{\partial v}{\partial P}\right)_T$$

by the existence of a TMD line. In the above equation, $v \equiv V/N$, the specific volume. We consider a path in the (P,T) projection along which the coefficient of thermal expansion α_P does not change, i.e.,

$$\alpha_P \equiv \frac{1}{v}\left(\frac{\partial v}{\partial T}\right)_P = \text{const.}$$

Thus, the condition for this path is

$$d\alpha_P = 0 = \left(\frac{\partial \alpha_P}{\partial T}\right)_P dT + \left(\frac{\partial \alpha_P}{\partial P}\right)_T dP. \tag{1}$$

Substituting for α_P in the right-hand side (rhs) of Eq. (1) we have

$$0 = \left(-\alpha_P^2 + \frac{1}{v}\frac{\partial^2 v}{\partial T^2}\right)dT + \left(K_T\alpha_P + \frac{1}{v}\frac{\partial^2 v}{\partial p\,\partial T}\right)dP, \tag{2}$$

from which we obtain

$$\left(\frac{dP}{dT}\right)_{d\alpha_P=0} = \frac{\alpha_P^2 - (1/v)(\partial^2 v/\partial T^2)}{K_T\alpha_P + (1/v)(\partial^2 v/\partial P\,\partial T)}. \tag{3}$$

Along the TMD line, where $\alpha_P = 0$,

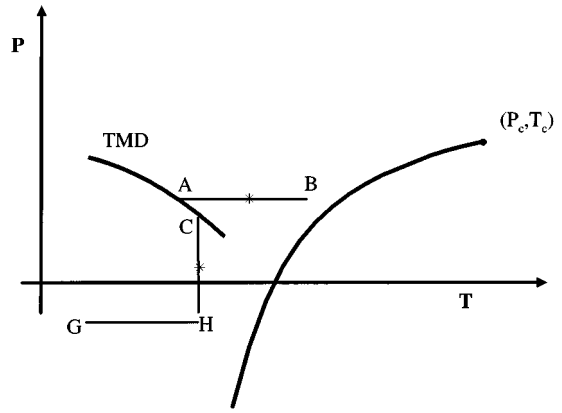

FIG. 2. Figure showing the paths to consider for analyzing the nonretracing scenario. The two asterisks indicate the points of K_T minimum (along path AB) and K_T extremum (along path CH).

$$\left(\frac{dP}{dT}\right)_{d\alpha_P=0}=\left(\frac{dP}{dT}\right)_{\mathrm{TMD}},$$

and thus, the slope of the TMD locus is

$$\left(\frac{dP}{dT}\right)_{\mathrm{TMD}}=-\frac{\left(\frac{\partial^2 v}{\partial T^2}\right)}{\left(\frac{\partial^2 v}{\partial P\partial T}\right)}. \tag{4}$$

We next calculate the temperature dependence of K_T at constant pressure,

$$\left(\frac{\partial K_T}{\partial T}\right)_P=-\frac{1}{v}\frac{\partial^2 v}{\partial P\partial T}+\frac{1}{v^2}\left(\frac{\partial v}{\partial T}\right)_P\left(\frac{\partial v}{\partial P}\right)_T \tag{5}$$

$$=-\left[\frac{1}{v}\frac{\partial^2 v}{\partial P\partial T}+K_T\alpha_P\right]. \tag{6}$$

Again, if we consider a point (P,T) with $\alpha_P=0$,

$$\left(\frac{\partial K_T}{\partial T}\right)_{P,\mathrm{TMD}}=-\frac{1}{v}\frac{\partial^2 v}{\partial P\partial T}. \tag{7}$$

Comparing Eq. (4) and Eq. (7), we find

$$\left(\frac{\partial K_T}{\partial T}\right)_{P,\mathrm{TMD}}=\frac{1}{v}\frac{\partial^2 v/\partial T^2}{(\partial P/\partial T)_{\mathrm{TMD}}}. \tag{8}$$

Equation (8) is a particularly interesting relation between the temperature dependence of K_T and the slope of the TMD line in the P,T plane. Indeed, Eq. (8) shows that along the TMD line, the signs of $(\partial K_T/\partial T)_{P,\mathrm{TMD}}$ and $(\partial P/\partial T)_{\mathrm{TMD}}$ are the same (since $\partial^2 v/\partial T^2>0$ at the TMD) and their magnitudes are inversely proportional. Where the TMD has negative slope in the (P,T) plane, K_T increases on cooling. Thus, in an anomalous liquid such as water, the increase in isothermal compressibility upon cooling is inseparably related to the presence of a negatively sloped TMD. Moreover, if the TMD intersects the TEC locus, the TMD becomes infinitely

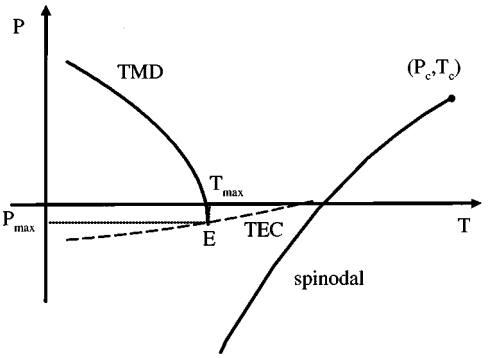

FIG. 3. Intersection of the TMD with the TEC locus (K_T extrema locus). Also shown is the liquid-gas spinodal line, starting at the critical point (P_c,T_c). The dashed line is the TEC locus, while the full line is the TMD line. Point E, with coordinates $P_{\max},T_{\max}$, is the point at which $(\partial P/\partial T)_{\mathrm{TMD}}$ is infinite.

sloped, while a zero sloped TMD implies $(\partial K_T/\partial T)_{P,\mathrm{TMD}}\to\infty$ (as is the case in the retracing spinodal scenario).

B. Analysis of the nonretracing spinodal scenario

We base our thermodynamic analysis on two assumptions: (i) the liquid under investigation has somewhere in the (P,T) plane a TMD line with a negative slope, and (ii) the liquid-gas spinodal is not retracing.

We consider the general behavior of the TMD and TEC lines, knowing that in a finite window of the (P,T) plane the TMD locus is negatively sloped and that the liquid-gas spinodal is not retracing. We also assume that the TMD line lies in the liquid region, i.e., that all the temperatures at which the TMD line is observed are less than the liquid-gas critical point.

We begin by noting that at any pressure there exists a range of intermediate temperatures [16] where $(\partial K_T/\partial T)_P$ is positive (e.g., point B in Fig. 2) [17]. Along the negatively-sloped TMD line, such as point A in Fig. 2, $(\partial K_T/\partial T)_P$ is negative. Hence, along the path from A to B, excluding the possibility of a discontinuity in $(\partial K_T/\partial T)_P$, there must be a point, denoted by an asterisk in Fig. 2, at which K_T is at a minimum.

We next consider the behavior of K_T along a path at constant pressure (e.g., GH in Fig. 2). Because K_T diverges at the spinodal, $(\partial K_T/\partial T)_P$ must be positive at H. At point C, which is on the TMD, it follows from Eq. (8) that $(\partial K_T/\partial T)_P$ is negative. Thus, excluding the possibility of a discontinuity in $(\partial K_T/\partial T)_P$, there must exist a point along the path CH at which $(\partial K_T/\partial T)_P=0$.

Given the assumptions that the TMD locus does not extend beyond T_c (i.e., that the TMD line is observed only in the liquid state) and that there is no retracing behavior of the spinodal, it is inevitable that the TMD locus and the locus of K_T extrema meet (point E in Fig. 3). At this point, in accord with Eq. (8), the slope of the TMD locus is infinite. To obtain the local behavior near E, the point at which the TMD line and the TEC locus meet, we study the Taylor series of $v-v_E$ as a function of $P-P_E$ and $T-T_E$, keeping the lowest order terms in $P-P_E$, $T-T_E$ and their cross terms. From such local analysis we obtain the three possibilities

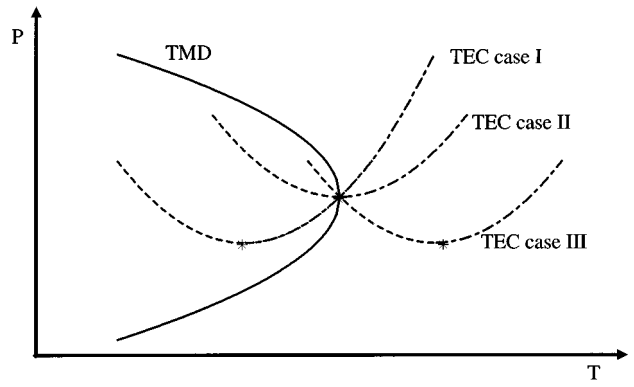

FIG. 4. The three possible cases when the TEC locus intersects the TMD line. The dashed part of each TEC locus indicates K_T maxima, while the dot-dashed part indicates points of K_T minima.

shown in Fig. 4, depending on whether the point E is a K_T minimum, a K_T maximum, or an inflection. Thus, when the spinodal is not retracing, the TMD line must change slope in the (P,T) plane upon intersecting the line of K_T extrema. Further, in all cases, we obtain a locus of K_T maxima below the TMD, though in case I (see Fig. 4), the temperature where the K_T extremum becomes a K_T maximum could be $T=0$.

To analyze the behavior of the specific heat at constant pressure, we consider the relation

$$c_P(T,v)-c_P^0(T)=T\int_\infty^v\left(\frac{\partial^2 P}{\partial T^2}\right)_v dv-T\frac{(\partial P/\partial T)_v^2}{(\partial P/\partial v)_T}-k_B, \tag{9}$$

where c_P^0 is the ideal gas specific heat. The second term in the rhs of the above expression is proportional to K_T. Hence, as demanded by thermodynamic consistency, c_P would diverge if K_T diverges, as at the liquid-gas spinodal. Even when K_T is not divergent, anomalous increases in c_P upon cooling, such as are observed in water [18], can result simply from the anomalous temperature dependence of K_T.

In summary, our analysis in this section indicates that without any assumptions about singular behavior, the shape of the TMD dictates the behavior of the compressibility in the vicinity of the TMD and that for a negatively sloped TMD, the compressibility necessarily increases on lowering temperature. In the absence of a retracing spinodal, we showed that the TMD has to retrace and that at temperatures sufficiently below the TMD, a locus of K_T maxima exists. Thus, broad thermodynamic features of anomalous behavior can neither be used to support singular behavior nor to distinguish between scenarios involving singularities and those that do not.

III. LATTICE MODEL

We present in this section a lattice model that exhibits behavior qualitatively similar to that observed in molecular dynamics simulations of water [7]. The model, however, does not exhibit any low temperature singular feature [19]. Thus, it serves as a demonstration of a nonsingular thermodynamic scenario that is consistent with observed properties of water. At the same time, a comparison of its properties with the predictions of the critical point scenario may be useful in distinguishing anomalous behavior that arises in water specifically due to the presence of a critical point and anomalous behavior that is not intimately related to singular behavior.

If we compare the configuration of a water molecule with strong hydrogen bond (HB) interactions with that of a water molecule with weak interactions, we find that the former defines a state of low local energy, entropy, and density (corresponding in water, for example, to the formation of a strong, linear, HB) while the latter defines a state of high local energy, entropy, and density [20]. When a strong HB forms, a lowering of energy arises due to the bonding interactions, and there is a reduction of entropy since HB's can form only when the interacting molecules are in specific orientations relative to each other; in addition, HB interactions lead to a loose packed geometric arrangement causing a lowering of the local density. In the following we will refer to the low energy, density, and entropy state as the HB-state and the high energy, density, and entropy state as the non-HB-state (NHB). Although the terminology is water-specific, the description has, in principle, broader validity.

These features have in the past been incorporated in lattice-gas models [20–22] defined in terms of conventional occupancy variables ($n=0$ or $n=1$) representing the molecules and Potts variables σ representing the orientational states of the molecules. These models have been solved approximately, the approximations arising from the manner in which the Potts variables are handled and from the mean field approximation used for obtaining the free energy. The different volumes for HB and NHB configurations have been taken into account by defining nearest and next-nearest neighbor interactions, corresponding to NHB and HB interactions, respectively.

One of the serious problems in adapting lattice-gas models to studying anomalous fluids lies in the treatment of volumes. For a simple system, configurations in a *condensed* state (in the sense of maximal interactions between atoms or molecules) and configurations with high density are synonymous. However, the characteristic feature of anomalous fluids is the very fact that in the *condensed* phase (i.e., when molecules interact strongly with each other), the arrangements of molecules are *less* dense. This fact is usually attended to by defining stronger interactions for neighbors that are farther away from each other than the closest possible spacing. However, in doing so one introduces additional ordered states which may or may not be desirable. Specifically, previous lattice models with waterlike properties typically have low-density ordered phases which are identified with ice [20]. While the presence of this phase is a desirable property, if one wants to model disordered but low-density, low energy structures, the presence of a phase with long range order poses a problem. It is of considerable interest to model such energetically favorable disordered states.

Here we present a simple model, which defines the correlations between bonding energy and local volumes in a fashion well-suited to studying disordered, energetically favorable states. In addition, the present model also avoids the complicated geometries and the approximations of previous models. This is achieved by making the volumes of sites on the lattice variable (these volumes are usually held constant

in lattice models and the volume of the system is simply given by the number of sites).

Consider a simple cubic (square lattice in two dimensions) lattice. At each site i we define occupancy variables n_i such that $n_i=0$ if site i is unoccupied, $n_i=1$ if site i is occupied. In order to distinguish between the energies of strong HB's we first define an interaction term $-\epsilon n_i n_j$ between occupied neighbors, regardless of any requirement for HB formation. Thus we write the Hamiltonian as

$$\mathcal{H}=\mathcal{H}_{\mathrm{NHB}}+\mathcal{H}_{\mathrm{HB}}=-\epsilon\sum_{\langle ij\rangle} n_i n_j+\mathcal{H}_{\mathrm{HB}}, \tag{10}$$

where $\langle ij\rangle$ refers to nearest neighbors. In order to define $\mathcal{H}_{\mathrm{HB}}$, we introduce variables $\sigma_{i,j}$ for each occupied site i, where j refers to any of the neighbors with which a molecule at site i can interact. Thus, $\sigma_{i,j}$ defines the orientation of molecule i with respect to molecule j. The full orientational state of molecule i is given by $\sigma_{i,j_1},\sigma_{i,j_2},\ldots,\sigma_{i,j_\gamma}$ where $j_1,j_2,\ldots,j_\gamma$ are the neighbors of i.

In principle, $\sigma_{i,j_1},\sigma_{i,j_2},\ldots,\sigma_{i,j_\gamma}$ are correlated quantities, because the orientation of a molecule along one arbitrary direction partially defines the orientation along all the other directions. Two extreme possibilities are as follows:

(1) $\sigma_{i,j}$ is an independent variable (for given i), i.e., the orientation of a molecule along j_1 is not correlated with the orientation along j_2.

(2) $\sigma_{i,j_1},\sigma_{i,j_2},\ldots,\sigma_{i,j_\gamma}$ are fully correlated variables, in which case we cannot change, e.g., σ_{i,j_1} without changing σ_{i,j_2}. In this limit we may represent the orientational state of molecule i with just one variable σ_i, i.e., $\sigma_{i,j_1}=\sigma_{i,j_2}=\cdots=\sigma_{i,j_\gamma}=\sigma_i$.

From a physical or geometric point of view, the situation is mixed. We make the former idealization in order to define our model Hamiltonian, keeping in mind that the behavior of the system is dependent on the idealization chosen.

We define $\sigma_{i,j}=\sigma_{j,i}$ to be the condition that i and j are properly oriented for HB formation. If the $\sigma_{i,j}$ have a range of possible values ($=1,2,\ldots,q$), it is clear that the relative entropy (in terms of the available number q of microstates) for HB's is lower than the number of microstates for NHB by a factor $\ln(q)$. Thus, defining the energy change on HB formation to be $-J$, we write

$$\mathcal{H}_{\mathrm{HB}}=-J\sum_{\langle ij\rangle} n_i n_j \delta_{\sigma_{i,j},\sigma_{j,i}}. \tag{11}$$

Finally we must quantify the change in local density as a result of HB formation. To do this, we first express the total volume V of the system as the sum of specific volumes V_i of sites i. The specific volumes V_i are in turn expressed in terms of contributions $b_{i,j}$ that depend on the interaction state between sites i and j. Thus,

$$V=\sum_i V_i\equiv\sum_{\langle i,j\rangle} b_{i,j}. \tag{12}$$

When i has a HB interaction with j, the local volume $b_{i,j}$ increases, leading to a larger specific volume V_i.

Clearly, one cannot represent arbitrary configurations with variable neighbor separations on a simple cubic lattice in a consistent fashion. Thus, we use the lattice geometry simply as a reference topology for defining interacting neighbors and calculate the volume of the system as the expectation value of variables $b_{i,j}$. For simplicity we define two possible values for $b_{i,j}$. (i) $b_{i,j}=b$ for NHB states and when n_i or $n_j=0$; (ii) $b_{i,j}=b+\delta b$ for HB states. Thus

$$\begin{aligned} V&=\sum_{\langle i,j\rangle} b_{i,j}=\sum_{\langle i,j\rangle}(b+\delta b n_i n_j \delta_{\sigma_{i,j},\sigma_{j,i}})\\ &=Nv_0+\delta b\sum_{\langle i,j\rangle} n_i n_j \delta_{\sigma_{i,j}\sigma_{j,i}}, \end{aligned} \tag{13}$$

where N is the number of lattice sites, $v_0\equiv\gamma b/2$, and γ is the coordination number. Thus we can write the system Hamiltonian $\mathcal{H}$ and "enthalpy" W (quotes because the enthalpy is the equilibrium average of the function below) as

$$\mathcal{H}=-\epsilon\sum_{\langle ij\rangle} n_i n_j - J\sum_{\langle ij\rangle} n_i n_j \delta_{\sigma_{i,j}\sigma_{j,i}}, \tag{14}$$

$$\begin{aligned} W=\mathcal{H}+PV&=-\epsilon\sum_{\langle ij\rangle} n_i n_j+P\frac{N\gamma b}{2}\\ &\quad-(J-P\delta b)\sum_{\langle ij\rangle} n_i n_j \delta_{\sigma_{i,j}\sigma_{j,i}}. \end{aligned} \tag{15}$$

In order to evaluate the partition function for this model, we must sum the appropriate Boltzmann weight over all values of n_i and $\sigma_{i,j}$. In doing so, however, the number of molecules as well as the volume of the system are variables. Thus the appropriate Boltzmann weight is $e^{-\beta(\mathcal{H}+PV-\mu N)}$ and the independent variables of this ensemble are (P,μ,T). The thermodynamic potential defined with (P,μ,T) is, however, identically zero, since $U-TS+PV-\mu N=0$. Nevertheless, it is possible to carry out the partition function evaluation and derive equilibrium properties in this ensemble. The fact that the partition function Γ is identically equal to 1 simply provides the additional relationship we require in order to evaluate dependent variables in this ensemble. We demonstrate the partition function evaluation for the exactly solvable one-dimensional case in Appendix A. In what follows, we shall show that the partition function evaluation is easily reduced to that of a simple lattice gas, and perform the evaluation of thermodynamic properties in the mean field approximation, which is sufficiently accurate for our purposes and further yields well-defined spinodals, which are significant elements of the phase behavior we wish to analyze.

Before performing a mean field calculation, we perform a trace of the partition function over the σ variables. In this model it is possible to perform an exact trace since the relevant variables for each bond are independent. Thus

$$\Gamma \equiv 1 = \sum_{n,\sigma} \exp\left[-\beta \left(W - \mu \sum_i n_i \right) \right] \tag{16}$$

$$= e^{-\beta P V_0} \sum_n \exp\left(\beta \epsilon \sum_{\langle ij \rangle} n_i n_j + \beta \mu \sum_i n_i \right) \times \sum_\sigma \exp\left(\beta J_P \sum_{\langle ij \rangle} n_i n_j \delta_{\sigma_{i,j}\sigma_{j,i}} \right) \tag{17}$$

with $J_P = J - P\delta b$ and $V_0 = N\gamma b/2$. Defining

$$B_{i,j}(\epsilon,\mu) = \exp\left(\beta \epsilon \sum_{\langle i,j \rangle} n_i n_j + \beta \mu \sum_i n_i \right), \tag{18}$$

we can write

$$e^{\beta P V_0} = \sum_n B_{i,j}(\epsilon,\mu) \times \prod_{\langle i,j \rangle} \sum_{\sigma_{i,j},\sigma_{j,i}} [1 + (e^{\beta J_P} - 1) n_i n_j \delta_{\sigma_{i,j},\sigma_{j,i}}] \tag{19}$$

$$= \sum_n B_{i,j}(\epsilon,\mu) \prod_{\langle ij \rangle} q^2 \left(1 + \frac{1}{q}(e^{\beta J_P} - 1) n_i n_j \right). \tag{20}$$

Since we have a factor $q^{\gamma/2}$ for each occupied site, we get

$$e^{\beta P V_0} = \sum_n e^{\beta \epsilon' \Sigma_{\langle i,j \rangle} n_i n_j + \beta \mu' \Sigma_i n_i} \equiv e^{-\beta \Omega} \tag{21}$$

with $\epsilon' = \epsilon + \delta J_P$; $\delta J_P = k_B T \ln[1 + 1/q(e^{\beta J_P} - 1)]$ and $\mu' = \mu + \gamma k_B T \ln(q)$.

The rhs in the previous equation is identical to the grand canonical partition function for a simple lattice gas. Hence we can evaluate the mean field "free energy" Ω in the usual way in the mean field approximation. Defining the number density $n \equiv M/N$, where the number of occupied sites $M \equiv \Sigma_i n_i$, we obtain

$$\frac{\Omega}{N} = -\epsilon'' n^2 - \mu' n + k_B T [n \ln(n) - (1-n)\ln(1-n)] \tag{22}$$

with $\epsilon'' = \gamma \epsilon'/2$. Minimizing Ω/N with respect to density n we obtain

$$\mu' = -2\epsilon'' n + k_B T \ln \frac{n}{1-n}. \tag{23}$$

Thus, with n as an implicit function of (P,μ,T), we have

$$\frac{\Omega}{N} = \epsilon'' n^2 - k_B T \ln(n(1-n)). \tag{24}$$

Since Ω/N is equal to $-PV_0/N = -Pv_0$, we have

$$P v_0 = -\epsilon'' n^2 - k_B T \ln(1-n) \tag{25}$$

which is identical in form to the mean field equation of state of a simple lattice gas. However, $\epsilon'' = \epsilon''(P,T)$. Further we need an additional equation relating n to the volume per molecule, $v \equiv V/M (= V/Nn)$. To this end, we use the equation for μ' (which is the Gibbs free energy per molecule) and write

$$v = \frac{\partial \mu}{\partial P} = \frac{\partial \mu'}{\partial P} = -2n \frac{\partial \epsilon''}{\partial P} + \left[-2\epsilon'' + \frac{k_B T}{n - n^2} \right] \frac{\partial n}{\partial P}. \tag{26}$$

From Eq. (25) we obtain

$$\frac{\partial n}{\partial P} = \frac{v_0 + n^2(\partial \epsilon''/\partial P)}{k_B T/(1-n) - 2\epsilon'' n} = \frac{1}{n} \frac{v_0 + n^2(\partial \epsilon''/\partial P)}{k_B T/(n - n^2) - 2\epsilon''}. \tag{27}$$

Thus,

$$v = \frac{v_0}{n} - n \left(\frac{\partial \epsilon''}{\partial P} \right)_T. \tag{28}$$

It must be noted that given a value of (P,T) Eq. (25) has at most three solutions [ϵ'' is a constant for fixed (P,T)]. Further, Eq. (28) yields a unique value of v for a given value of n. Hence, at given (P,T) we find at most three solutions for v, which implies that there is no more than one van der Waals–like loop for each isotherm [23].

Equations (25) and (28) together define the equation of state for this model. Equation (28) may be inverted to write n in terms of v as follows:

$$n = \frac{v \pm [v^2 + 4v_0(\partial \epsilon''/\partial P)]^{1/2}}{-2\partial \epsilon''/\partial P}. \tag{29}$$

In addition to the thermodynamic quantities that may be calculated from the implicit equation of state above, we can also straightforwardly calculate a "microscopic" quantity of interest, namely the hydrogen bond probability. Considering Eq. (13) for the total volume of the system and noting that the sum $\Sigma_{\langle i,j \rangle} n_i n_j \delta_{\sigma_{i,j}\sigma_{j,i}}$ is equal to the total number of hydrogen bonds present, we can write the hydrogen bond probability p_b as

$$p_b(P,T) \equiv \frac{\Sigma_{\langle i,j \rangle} n_i n_j \delta_{\sigma_{i,j}\sigma_{j,i}}}{(N\gamma/2)} = \frac{2}{\gamma \delta b}(vn - v_0). \tag{30}$$

The ratio of the number of HB's present to the mean field estimate of the number of bonds actually present is given by

$$p_{\mathrm{HB}}(P,T) = P_b(P,T)/n^2. \tag{31}$$

While p_b is the more appropriate quantity in reference to percolation properties, p_{HB} is a better indicator of the degree of hydrogen bonding in the system.

IV. RESULTS

We have studied the equation of state derived above for a variety of parameters. For all parameter values, the generic behavior produced is very similar in that we always find a retracing TMD. Associated with the retracing TMD is the locus of compressibility extrema, TEC, which we find inter-

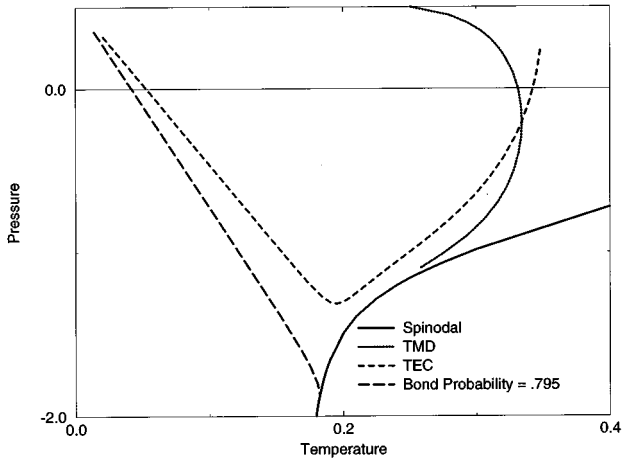

FIG. 5. Phase diagram for the lattice model showing the TMD line, spinodal, and the TEC line. The TEC meets the TMD at the retracting point. Note that below the T at which the K_T extrema locus displays a minimum, the extrema are maxima, while above they are minima. Also shown is the $p_b=0.795$ locus. Temperature is expressed in units of ϵ/k_B and pressure in units of ϵ/v_0.

sects the TMD with positive slope. The spinodal in the system is not retracing. The data shown are for the choice of parameters $\delta b/b=0.953$, $J/\epsilon=0.25$, $q=100$. The overall behavior is summarized in Fig. 5. Note that the TEC has a minimum in pressure at which point it changes from being a locus of compressibility minima to a locus of compressibility maxima. Thus, at low temperatures, one finds compressibility maxima along isobars. Also shown in the figure is the locus where $p_b=0.795$.

The compressibilities along various isobars are shown in Fig. 6. Note that the compressibility values at the maxima increase as the pressure is increased, with the maxima occurring at lower temperatures at higher pressures. However, at a fixed temperature, considering pressures above the TEC locus at that temperature, we find that the compressibility is indeed a decreasing function of pressure (e.g., at $T = 0.2$ in Fig. 6), consistently with the behavior of water. Further, the behavior seen of the compressibility maxima is consistent with the behavior seen in computer simulations [7].

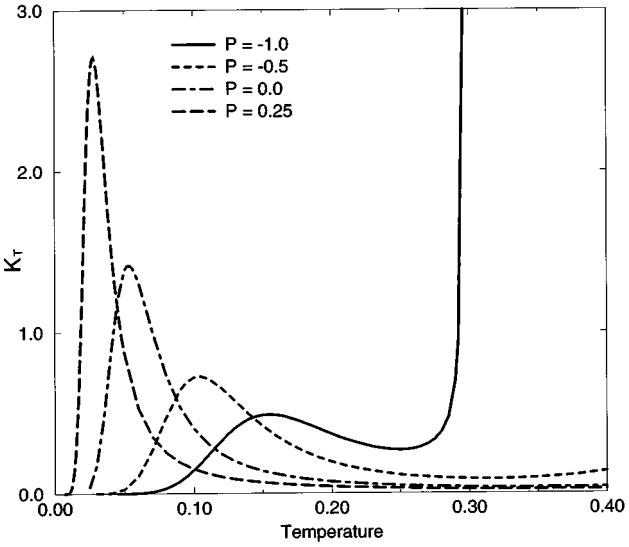

FIG. 6. Isobaric behavior of K_T for different pressures. At $P=-1.0$, K_T diverges as T approaches the spinodal temperature. Note that K_T remains finite at low temperatures. Temperature is expressed in units of ϵ/k_B, pressure in units of ϵ/v_0, and K_T in units of v_0/ϵ.

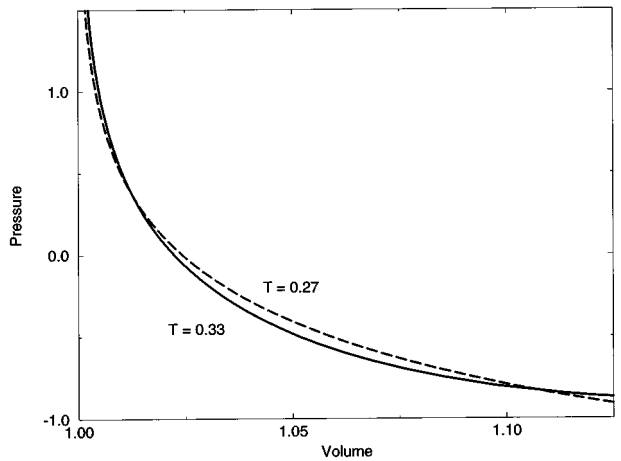

FIG. 7. High temperature isotherms which display no inflections. Volume is expressed in units of v_0 and pressure in units of ϵ/v_0. Temperature values labeling curves are in units of ϵ/k_B.

In making a qualitative comparison with simulation results of water, the behavior of isotherms is particularly interesting. Thus, we show two sets of isotherms, at relatively high temperatures in Fig. 7 and for very low temperatures in Fig. 8. Note that along the high T isotherms, the K_T extremum crossed is a compressibility minimum, while along the low T isotherms, the K_T extremum crossed is a compressibility maximum (see Fig. 5). It is interesting to note that the high temperature isotherms cross each other at two points which is an indication that there are two density maximum points along an isothermal path (i.e., retracing TMD). These isotherms, however, do not exhibit any inflections. Thus, these high temperature isotherms display the simplest possible behavior of isotherms which may still be consistent with the retracing TMD scenario.

Next we consider the low temperature isotherms shown in

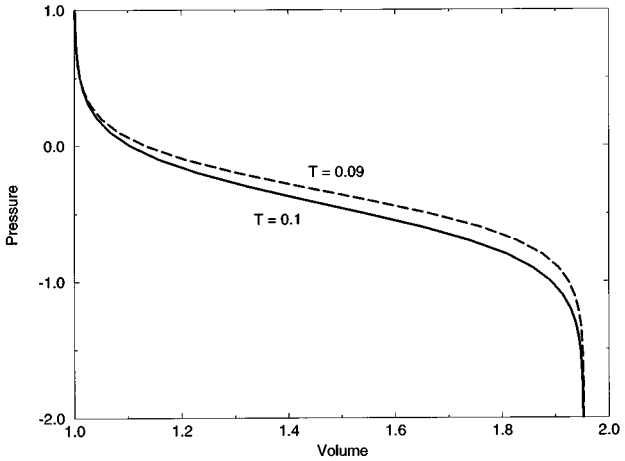

FIG. 8. Low-temperature isotherms displaying inflections. Volume is expressed in units of v_0 and pressure in units of ϵ/v_0. Temperature values labeling curves are in units of ϵ/k_B.

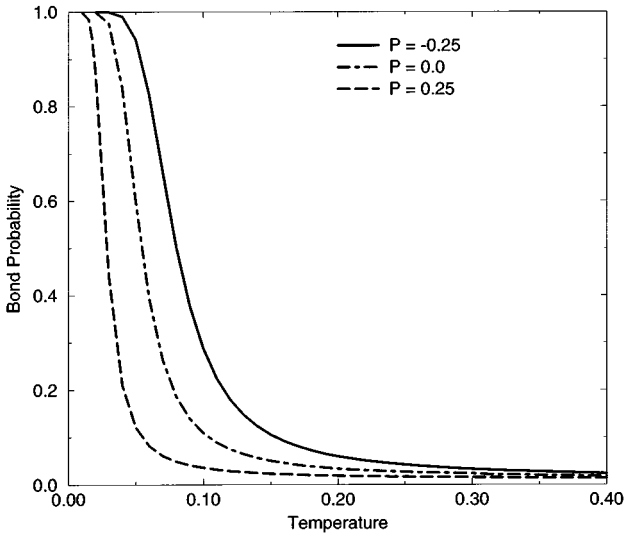

FIG. 9. Hydrogen bond probability as a function of temperature at various pressures. Temperature is expressed in units of ϵ/k_B and pressure in units of ϵ/v_0.

Fig. 8. These isotherms do indeed show inflections which get more pronounced as the temperature is lowered. However, as mentioned in the preceding section, these inflections do not develop into a critical point in this model. Thus, the low temperature isotherms provide the second simplest behavior consistent with the retracing TMD scenario. The presence of a critical point is a special case of the above.

Figure 9 shows the variation of the hydrogen bond probability p_b with temperature at three different pressures. The hydrogen bond probability is seen to approach unity at $T \rightarrow 0$, with higher values for lower pressures. The variation with pressure is seen more clearly in Fig. 10, where p_b is plotted for three different temperatures. From the (P,T) dependence of p_b, we may also calculate loci of constant p_b. We show one such locus ($p_b = 0.795$) in Fig. 5 [24].

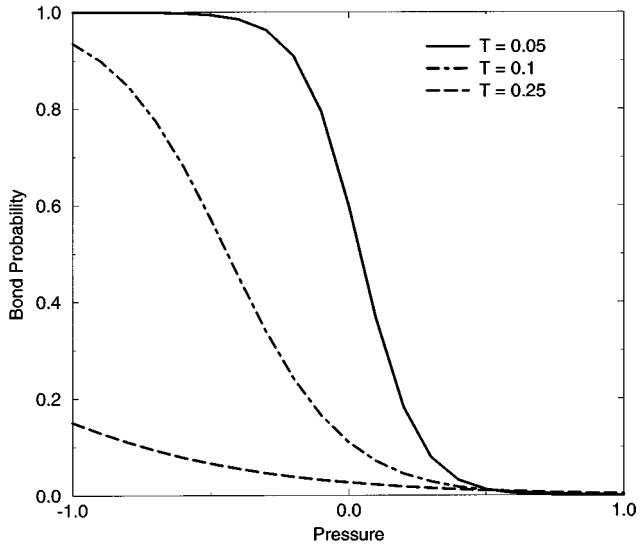

FIG. 10. Hydrogen bond probability as a function of pressure at various temperatures. Temperature is expressed in units of ϵ/k_B and pressure in units of ϵ/v_0.

V. DISCUSSION

We have presented thermodynamic arguments which result in two statements relevant to the behavior of any anomalous liquid, such as water, for which the density decreases on cooling below the TMD: (i) If an anomalous liquid exhibits a negatively sloped TMD, then the isothermal compressibility at constant pressure increases on decreasing the temperature. Thus, increases in compressibility are not *a priori* an indication of any singular behavior, as has been implicitly accepted in thermodynamic analyses of supercooled water. (ii) When the liquid does not exhibit a retracing spinodal, the TMD retraces to lower temperatures upon intersecting with the locus of compressibility extrema. Generally, the resulting phase diagram exhibits a locus of compressibility maxima along isobars. Hence, in the simplest interpretation of simulation data for supercooled water, one expects a line of compressibility maxima at low temperatures. Indeed, recent small angle x-ray scattering measurements of the low temperature structure factors [25] point to such behavior, which has been observed for other anomalous liquids [26–28]. The proposed metastable critical point scenario forms a special case, where the compressibility at points of the TEC locus either diverges (at the critical point) or is discontinuous (first order line).

Additionally, we presented a lattice model that demonstrates some observations of the thermodynamic analysis, exhibiting behavior free of low temperature singularities. A comparison of the behavior of this model with simulation data for water and the critical point interpretation imposes constraints on what experimental results may be viewed as supporting the critical point scenario.

It is interesting to note that the model described may be viewed as a thermodynamic realization of some basic features of the percolation model of Stanley and Teixeira [29], which does indeed predict the presence of compressibility maxima at low temperatures (i.e., no thermodynamic singularities). The interpretation of thermodynamic properties in this model in terms of percolation quantities remains to be studied; in particular, the relevant percolation threshold is not known. It would be interesting to study the relation between the compressibility increase, which in our model is related to the transformation of weak bonds to strong bonds, and the approach of the appropriate percolation transition [30].

The scenario described in this paper is the simplest one that is consistent with experimental observations. The significance of our work is not to have proved a particular scenario, but rather to provide a simpler explanation of experimental observations than those recently emphasized, and to suggest experiments [31] that are needed to validate or refute this interpretation.

One suggestion for future work that arises from the present results concerns dynamical properties. The apparent divergence of certain dynamical quantities has been used in tandem with the more ambiguous apparent divergences of thermodynamic quantities as indicating *thermodynamic* singularities at low temperatures in water. However, if a singularity-free scenario is capable of explaining satisfactorily the behavior of thermodynamic quantities, the dynamical phenomena then need an explanation that is independent of

the thermodynamic anomalies. Such an explanation has recently been suggested by Gallo *et al.* [32] who, based on molecular dynamics evidence, propose to interpret the extrapolated vanishing of the diffusion coefficient in supercooled water as due to an ideal glass transition as in the mode coupling theory [33] for supercooled liquids. A study of the dynamics of the lattice model presented here (or a more convenient reformulation) may help in addressing this issue.

ACKNOWLEDGMENTS

We thank Peter H. Poole, Robin J. Speedy, and Philipp Maass for useful discussions. P.G.D. gratefully acknowledges the financial support of the U.S. DOE, Division of Chemical Sciences, Office of Basic Energy Sciences (Grant No. DEFG02-87ER13714). H.E.S. acknowledges the National Science Foundation for financial support. F.S. acknowledges the support of the INFM-MURST and the GNSM-CNR.

APPENDIX A: ONE-DIMENSIONAL LATTICE: THE HAMILTONIAN AND THE ENTHALPY FUNCTIONS

For the one-dimensional lattice, the Hamiltonian and the enthalpy functions in Eq. (14) and Eq. (15) become

$$\mathcal{H}=-\epsilon\sum_i n_i n_{i+1}-J\sum_i n_i n_{i+1}\delta_{\sigma_{i,i+1}\sigma_{i+1,i}}, \tag{A1}$$

$$W=\mathcal{H}+PV=-\epsilon\sum_i n_i n_{i+1}+PV_0 -(J-P\delta b)\sum_i n_i n_{i+1}\delta_{\sigma_{i,i+1}\sigma_{i+1,i}}, \tag{A2}$$

where $V_0=Nv_0\equiv Nb'$. We also define $(J-P\delta b)\equiv J_P$. In the (P,μ,T) ensemble, the partition function is

$$\Gamma=e^{-\beta\Delta}\equiv 1=\sum_{n,\sigma} e^{-\beta(W-\mu\Sigma_i n_i)}, \tag{A3}$$

so that

$$\Gamma e^{\beta PV_0}=\sum_{n,\sigma} e^{-\beta\epsilon\Sigma_i n_i n_{i+1}+\beta(\mu/2)\Sigma_i(n_i+n_{i+1})} \times e^{\beta J_P\Sigma_i n_i n_{i+1}\delta_{\sigma_{i,i+1}\sigma_{i+1,i}}}. \tag{A4}$$

Defining

$$B_{i,i+1}(\epsilon,\mu)=e^{-\beta\epsilon\Sigma_i n_i n_{i+1}+\beta(\mu/2)\Sigma_i(n_i n_{i+1})}, \tag{A5}$$

we have

$$\Gamma e^{\beta PV_0}=\sum_n B_{i,i+1}(\epsilon,\mu)\sum_\sigma\prod_i e^{\beta J_P\Sigma_i n_i n_{i+1}\delta_{\sigma_{i,i+1}\sigma_{i+1,i}}} \tag{A6}$$

$$=\sum_n B_{i,i+1}(\epsilon,\mu)\prod_i\sum_{\sigma_{i,i+1},\sigma_{i+1,i}}[1+(e^{\beta J_P}-1) \times n_i n_{i+1}\delta_{\sigma_{i,i+1},\sigma_{i+1,i}}]. \tag{A7}$$

If for a given i, $n_i=n_{i+1}=1$, the sum $\Sigma_{\sigma_{i,i+1},\sigma_{i+1,i}}$ yields

$$[q^2+q(e^{\beta J_P}-1)n_i n_{i+1}]=q^2\left(1+\frac{1}{q}(e^{\beta J_P}-1)n_i n_{i+1}\right). \tag{A8}$$

For the full product Π_i, then, we can factor out $q^{2\Sigma_i n_i}$. Thus we can write

$$\Gamma e^{\beta PV_0}=\sum_n B_{i,i+1}(\epsilon,\mu)q^{2\Sigma_i n_i} \times\prod_i\left(1+\frac{1}{q}(e^{\beta J_P}-1)n_i n_{i+1}\right) =\sum_n B_{i,i+1}(\epsilon,\mu)e^{\beta 2T\ln(q)\Sigma_i n_i}e^{\beta\delta J_P\Sigma_i n_i n_{i+1}}, \tag{A9}$$

where $\delta J_P=T\ln[1+1/q(e^{\beta J_P}-1)]$. Thus,

$$\Gamma e^{\beta PV_0}=\sum_n e^{\beta^0\epsilon'\Sigma_i n_i n_{i+1}+\mu'/2\Sigma_i(n_i+n_{i+1})^0}, \tag{A10}$$

where $\epsilon'=\epsilon+\delta J_P$ and $\mu'=\mu+2T\ln(q)$. Defining

$$\prod_i U_{i,i+1}=e^{\beta[\epsilon'\Sigma_i n_i n_{i+1}+\mu'/2\Sigma_i(n_i+n_{i+1})]}, \tag{A11}$$

we obtain

$$\Gamma e^{\beta PV_0}=TrU^N, \tag{A12}$$

where

$$U=\begin{pmatrix} 1 & e^{\beta\mu'/2} \\ e^{\beta\mu'/2} & e^{\beta(\epsilon'+\mu')}\end{pmatrix}. \tag{A13}$$

If we define λ_+ and λ_- to be the larger and the smaller eigenvalues of U, respectively, we can write

$$TrU^N=\lambda_+^N+\lambda_-^N, \tag{A14}$$

which for $N\to\infty$ gives $TrU^N=\lambda_+^N$. Since $\Gamma=1$, we have

$$e^{\beta PV_0}=\lambda_+^N, \tag{A15}$$

from which we get $\beta Pb'=\ln(\lambda_+)$. The subscript + on λ_+ will be suppressed in the following. This relation defines, in contrast to usual partition function evaluations, a relationship between variables (P,μ,T). We shall use the above relation to define $\mu=\mu(P,T)$, which then defines the equilibrium Gibbs free energy per molecule. Thus, the volume per molecule v is given by

$$v=\frac{\partial\mu}{\partial P}=\frac{\partial\mu'}{\partial P}=T\frac{\partial\ln(y)}{\partial P}, \tag{A16}$$

where $y\equiv e^{\beta\mu'}$. Defining $x\equiv e^{\beta\epsilon'}$, we have

$$v=T\left[\frac{1}{y}\frac{\partial y}{\partial \lambda}\frac{\partial \lambda}{\partial P}+\frac{1}{y}\frac{\partial y}{\partial x}\frac{\partial x}{\partial P}\right]. \tag{A17}$$

From $\exp(\beta P b')=\lambda$, we find

$$\frac{\partial \lambda}{\partial P}=\beta b'\exp(\beta P b'). \tag{A18}$$

From

$$y=\frac{\lambda^2-\lambda}{(\lambda-1)x+1}, \tag{A19}$$

we have, after some algebra,

$$\frac{\partial y}{\partial \lambda}=\frac{x[\exp(\beta P b')-1]^2+2\exp(\beta P b')-1}{\{[\exp(\beta P b')-1]x+1\}^2}. \tag{A20}$$

Thus

$$\frac{1}{y}\frac{\partial y}{\partial \lambda}=\frac{x[\exp(\beta P b')-1]^2+2\exp(\beta P b')-1}{\exp(\beta P b')[\exp(\beta P b')-1]\{[\exp(\beta P b')-1]x+1\}}. \tag{A21}$$

Similarly,

$$\frac{1}{y}\frac{\partial y}{\partial x}=\frac{1-\exp(\beta P b')}{(\beta b' P-1)x+1}. \tag{A22}$$

From $\delta J_P=T\ln[1+1/q(e^{\beta J_P}-1)]$, $\epsilon'=\epsilon+\delta J_P$, we obtain

$$\frac{\partial x}{\partial P}=\frac{-\beta e^{\beta\epsilon'}\delta b}{q}\left[1+\frac{1}{q}(e^{\beta J_P}-1)\right]^{-1}. \tag{A23}$$

Substituting from Eqs. (A18), (A21), (A22), and (A23) in Eq. (A17), we have the equation of state for the system. Hence, we recover exact results for the one-dimensional lattice by using the property of the generalized ensemble, namely that the corresponding thermodynamic potential is identically zero.

[1] R. J. Speedy, J. Phys. Chem. **86**, 982 (1982).

[2] R. J. Speedy, J. Phys. Chem. **86**, 3002 (1982).

[3] P. G. Debenedetti and M. C. D'Antonio, J. Chem. Phys. **84**, 3339 (1986).

[4] P. G. Debenedetti and M. C. D'Antonio, J. Chem. Phys. **85**, 4005 (1986).

[5] M. C. D'Antonio and P. G. Debenedetti, J. Chem. Phys. **86**, 2229 (1987).

[6] P. G. Debenedetti and M. C. D'Antonio, AIChE J. **34**, 447 (1988).

[7] P. H. Poole, F. Sciortino, U. Essmann, and H. E. Stanley, Nature **360**, 324 (1992); For recent related work, see also P. H. Poole, F. Sciortino, T. Grande, H. E. Stanley, and C. A. Angell, Phys. Rev. Lett. **73**, 1632 (1994); H. Tanaka, Nature **380**, 328 (1996).

[8] P. H. Poole, F. Sciortino, U. Essmann, and H. E. Stanley, Phys. Rev. E **48**, 3799 (1993).

[9] In this paper, we refer to this behavior whereby the slope of the TMD changes sign as the *retracing TMD* behavior, and we call the thermodynamic scenarios consistent with this behavior *retracing TMD* scenarios.

[10] P. H. Poole, U. Essmann, F. Sciortino, and H. E. Stanley, Phys. Rev. E **48**, 4605 (1993).

[11] O. Mishima, L. D. Calvert, and E. Whalley, Nature **310**, 393 (1984).

[12] O. Mishima, L. D. Calvert, and E. Whalley, Nature **314**, 76 (1985).

[13] O. Mishima, J. Chem. Phys. **100**, 5910 (1994).

[14] M. A. Floriano, Y. P. Handa, D. D. Klug, and E. Whalley, J. Chem. Phys. **91**, 7187 (1993).

[15] T. L. Hill, *Statistical Mechanics* (Dover Publications, New York, 1987).

[16] This applies to the liquid phase or for the high density fluid when one considers pressures $P>P_c$.

[17] This can be seen as follows: consider a range of temperatures (a) below the critical temperature for $P=P_c$, (b) below the spinodal temperature for $P<P_c$, and (c) below the temperature along the critical isochore for $P>P_c$; in each case, at constant pressure, K_T is an increasing function of temperature.

[18] D. H. Rasmussen, A. P. Mackenzie, C. A. Angell, and J. C. Tucker, Science **181**, 342 (1973); C. A. Angell, J. Shuppert, and J. C. Tucker, J. Phys. Chem. **77**, 3092 (1973).

[19] The model does not *prove* that there are no low temperature singularities in water; only experiments can do that. Because such experiments must probe the behavior of a highly supercooled liquid, they are especially difficult. Given this situation, theoretical calculations are useful in two ways. First, they provide thermodynamically consistent scenarios with stringent constraints on the allowed behavior of observable quantities (e.g., a negatively-sloped TMD implies that the compressibility must increase upon cooling). Second, they suggest what must be measured in order to test the theoretical predictions. For example, volumetric and calorimetric measurements of glassy water at different pressures will yield information on the continuity of states between supercooled and glassy water, and hence on the presence, or absence, of the proposed spinodal, critical point, etc.

[20] S. Sastry, F. Sciortino, and H.E. Stanley, J. Chem. Phys. **98**, 9863 (1993).

[21] M. Sasai, J. Chem. Phys. **93**, 7329 (1990); Bull. Chem. Soc. Jpn. **97**, 6292 (1993).

[22] S. S. Borick, P. G. Debenedetti, and S. Sastry, J. Phys. Chem. **99**, 3781 (1995).

[23] The absence of a second critical point, however, is not just an artifact of the mean field calculation, but a feature of the model.

[24] This value corresponds to the percolation threshold of four bonded molecules on an ice lattice [30], which plays a special role in the percolation model of Stanley and Teixeira [29].

[25] Y. Xie, K. F. Ludwig, Jr., G. Morales, D. E. Hare, and C. M.

Sorensen, Phys. Rev. Lett. **71**, 2050 (1993).
[26] Y. Tsuchiya, J. Phys. Soc. Jpn. **60**, 227 (1991).
[27] Y. Tsuchiya, J. Phys. Soc. Jpn. **60**, 960 (1991).
[28] Y. Tsuchiya, J. Phys. Condens. Matter **3**, 3163 (1991).
[29] H. E. Stanley and J. Teixeira, J. Chem. Phys. **73**, 3404 (1980).
[30] R. L. Blumberg, H. E. Stanley, A. Geiger, and P. Mausbach, J. Chem. Phys. **80**, 5230 (1984).
[31] An example would be volumetric and calorimetric measurements of glassy water at different pressures; these yield data on the continuity of states between supercooled and glassy water that validate or falsify the scenario described by this model.
[32] P. Gallo, F. Sciortino, P. Tartaglia, and S. -H. Chen (unpublished).
[33] W. Götze and L. Sjögren, Rep. Prog. Phys. **55**, 241 (1992).